

ARTICLE

A comprehensive evaluation in clinic and physiologically-based pharmacokinetic modeling and simulation to confirm lack of cytochrome P450-mediated drug–drug interaction potential for pomotrelvir

Ziping Yang¹ | Nathalie Rioux² | Ludwig Vincent² | Hannah M. Jones² |
David Cha¹ | Andrew Plummer¹ | David Wilfret¹  | Brian P. Kearney¹

¹Pardes Biosciences, Inc., Carlsbad, California, USA

²Certara, Princeton, New Jersey, USA

Correspondence

Ziping Yang, Pardes Biosciences, Inc.,
2173 Salk Ave, Suite 250, PMB 052,
Carlsbad, CA 92008, USA.

Email: prdspublications@pardesbio.com

Abstract

Pomotrelvir is a new chemical entity and potent direct-acting antiviral inhibitor of the main protease of coronaviruses. Here the cytochrome P450 (CYP)-mediated drug–drug interaction (DDI) potential of pomotrelvir was evaluated for major CYP isoforms, starting with in vitro assays followed by the basic static model assessment. The identified CYP3A4-mediated potential DDIs were evaluated clinically at a supratherapeutic dose of 1050 mg twice daily (b.i.d.) of pomotrelvir, including pomotrelvir coadministration with ritonavir (strong inhibitor of CYP3A4) or midazolam (sensitive substrate of CYP3A4). Furthermore, a physiologically-based pharmacokinetic (PBPK) model was developed within the Simcyp Population-based Simulator using in vitro and in vivo information and validated with available human pharmacokinetic (PK) data. The PBPK model was simulated to assess the DDI potential for CYP isoforms that pomotrelvir has shown a weak to moderate DDI in vitro and for CYP3A4 at the therapeutic dose of 700 mg b.i.d. To support the use of pomotrelvir in women of childbearing potential, the impact of pomotrelvir on the exposure of the representative oral hormonal contraceptive drugs ethinyl estradiol and levonorgestrel was assessed using the PBPK model. The overall assessment suggested weak inhibition of pomotrelvir on CYP3A4 and minimal impact of a strong CYP3A4 inducer or inhibitor on pomotrelvir PK. Therefore, pomotrelvir is not anticipated to have clinically meaningful DDIs at the clinical dose. These comprehensive in vitro, in clinic, and in silico efforts indicate that the DDI potential of pomotrelvir is minimal, so excluding patients on concomitant medicines in clinical studies would not be required.

This is an open access article under the terms of the [Creative Commons Attribution-NonCommercial-NoDerivs](https://creativecommons.org/licenses/by-nc-nd/4.0/) License, which permits use and distribution in any medium, provided the original work is properly cited, the use is non-commercial and no modifications or adaptations are made.

© 2023 The Authors. *CPT: Pharmacometrics & Systems Pharmacology* published by Wiley Periodicals LLC on behalf of American Society for Clinical Pharmacology and Therapeutics.

Study Highlights

WHAT IS THE CURRENT KNOWLEDGE ON THE TOPIC?

The most prescribed oral treatment for coronavirus disease 2019 (COVID-19) in the United States, ritonavir-boosted nirmatrelvir, is contraindicated for coadministration with a number of commonly prescribed drugs because of the potential for drug–drug interactions (DDIs). Pomotrelvir is a new chemical entity being developed for treatment of COVID-19.

WHAT QUESTION DID THIS STUDY ADDRESS?

The cytochrome P450 (CYP) enzyme-mediated DDI potential was evaluated in in vitro and clinical studies. These results, along with human pharmacokinetic data from the first-in-human study, were used to develop a physiologically-based pharmacokinetic (PBPK) model to simulate the DDI potential for pomotrelvir as a perpetrator for various CYP enzyme activities and as a victim of CYP3A4.

WHAT DOES THIS STUDY ADD TO OUR KNOWLEDGE?

Pomotrelvir's lack of potential for clinically meaningful CYP enzyme-mediated DDIs in humans was predicted early in its development. These results supported the decision to remove typical restrictions on the use of concomitant medications from the phase II trial's inclusion/exclusion criteria.

HOW MIGHT THIS CHANGE DRUG DISCOVERY, DEVELOPMENT, AND/OR THERAPEUTICS?

The favorable DDI profile suggests a potential advantage of pomotrelvir over commonly prescribed COVID-19 oral treatments. The strategy of applying PBPK modeling and simulation allowed for early DDI potential prediction and avoided the unnecessary exclusion of patients in clinical trials and potentially additional clinical DDI trials, thereby reducing unnecessary exposure to DDI study drugs in healthy volunteers.

INTRODUCTION

Although the worst outcomes from the ongoing coronavirus disease 2019 (COVID-19) endemic have been mitigated by vaccines, the variable uptake of vaccines and the continued emergence of new and highly transmissible variants, for which currently available vaccines may be less effective, have led to the need for direct-acting antiviral treatments effective against severe acute respiratory syndrome coronavirus 2 (SARS-CoV-2) infections.¹ Although new therapeutics for COVID-19 have improved patient outcomes, additional treatment options are needed, especially in patients who take medications for comorbid conditions.^{2,3} Concomitant use of the most commonly prescribed oral treatment within the United States, ritonavir-boosted nirmatrelvir (PAXLOVID™), is contraindicated with a number of commonly prescribed drugs that are highly dependent on cytochrome P450 (CYP) 3A for clearance or are potent CYP3A inducers.^{4,5}

Pomotrelvir (PBI-0451) is an orally bioavailable, direct-acting, antiviral inhibitor of the main protease of coronaviruses and is being developed as a stand-alone agent for the treatment of COVID-19.⁶ A phase I, first-in-human

(FIH) ([ClinicalTrials.gov: NCT05011812](https://clinicaltrials.gov/ct2/show/study/NCT05011812)) study showed that pomotrelvir is well tolerated, with good oral bioavailability and dose-linear, single- and multiple-dose pharmacokinetic (PK) exposures over a >20-fold dose range when administered with food.⁷

In the past two decades, physiologically-based PK (PBPK) modeling has become an accepted approach to inform drug–drug interaction (DDI) risk and reduce DDI studies. The use of PBPK modeling is encouraged by the regulatory authorities and the framework to include PBPK in the new drug application submission is documented in guidance from the US Food and Drug Administration (FDA).⁸ Herein, a comprehensive evaluation of the CYP enzyme-mediated DDI potential of pomotrelvir in in vitro and clinical studies along with PBPK modeling is presented.

METHODS

In vitro assays

The DDI potential of pomotrelvir was evaluated in standard in vitro experiments including CYP enzyme

phenotyping, inhibition, and induction studies, followed by the assessment using the basic static model as described in the FDA's Guidance.⁹ (Detailed methods are in Appendix S1.)

Clinical DDI study with midazolam and ritonavir

Three DDI cohorts were included in the FIH study ([ClinicalTrials.gov: NCT05011812](https://clinicaltrials.gov/ct2/show/study/NCT05011812)) to evaluate the impact of multiple doses of pomotrelvir on the PK of midazolam (a sensitive probe substrate for CYP3A4¹⁰) and the impact of coadministering ritonavir (a potent, mechanism-based inhibitor of CYP3A4¹¹) on the PK of pomotrelvir. Informed consent was obtained from all individual participants included in the study before any screening procedures. The study protocol was reviewed and approved by the institutional review board at the study site (Auckland City Hospital, Auckland, New Zealand).

Participants

Eight healthy adults (with an approximately even distribution between males and nonpregnant, nonlactating females) aged between 18 and 59 years with body mass indexes ≥ 19.0 and $\leq 30.0 \text{ kg/m}^2$ were enrolled in each of the DDI cohorts. Participants were in good general health as determined by the investigator at a screening evaluation performed no more than 28 days before the scheduled first dose. Medications and food contraindicated with midazolam or ritonavir were prohibited for the participants in these cohorts.

Study design for midazolam DDI cohort

This was a crossover design with 1 mg midazolam oral solution (1 mg/mL) administered alone on Day 1 and coadministered with a supratherapeutic dose of pomotrelvir at 1050 mg (three 350 mg tablets, twice daily [b.i.d.] from Days 2 through 11) on Days 6 and 11 under fed conditions. All treatments were administered with 240 mL of water following an overnight fast and immediately after fully completing a standard meal. Blood samples for PK profiles (18 timepoints, up to 24 h postdose) were collected on Days 1, 6, and 11 for midazolam and Days 6 and 11 for pomotrelvir, also at the time corresponding to the morning predose on Days 4 and 8 for pomotrelvir. Plasma concentrations of midazolam and 1-hydroxy-midazolam (1-OH-midazolam) were determined using a validated liquid chromatography with tandem mass spectrometry

(LC-MS/MS) method with a quantitation dynamic range from 0.1 to 100 ng/mL.

Study design for ritonavir DDI cohorts

Two cohorts with 100 mg ritonavir once daily oral coadministration with pomotrelvir suspension at a single dose of 20 mg or multiple doses of 50 mg (once daily for 10 days). The PK of pomotrelvir from these two DDI cohorts was compared with that from the single dose of 100 mg pomotrelvir suspension alone. The treatment procedure was the same as that for the midazolam DDI cohort. Blood samples for PK profiles (18 timepoints, up to 24 h postdose) were collected on Days 1, 5, and 10 and at the time corresponding to the morning predose on Days 4 and 8, if applicable, for pomotrelvir and ritonavir. Plasma concentration of pomotrelvir was determined using a validated LC-MS/MS method with a quantitation dynamic range from 10 to 10,000 ng/mL.

PK and statistical analysis

All PK and statistical analyses were conducted by using SAS Version 9.4 or higher (SAS Institute) or Phoenix WinNonlin Version 8.3 or higher (Certara). The PK analyses of plasma midazolam, 1-OH-midazolam, and pomotrelvir were performed by a noncompartmental method, and the PK parameters, including maximum observed concentration (C_{\max}), area under the curve [AUC] from time 0 to the last quantifiable concentration (AUC_{last}), and AUC from time 0 to infinity (AUC_{inf}), were calculated. The effect of pomotrelvir on midazolam PK was assessed by comparing midazolam and 1-OH-midazolam plasma exposure (C_{\max} and AUC) on Day 1 versus 6 and Day 1 versus 11. To assess the effect of ritonavir on pomotrelvir PK, the dose-normalized plasma exposure of pomotrelvir (C_{\max}/dose and AUC/dose) was compared between the treatments of pomotrelvir alone (100 mg, single dose) and coadministered with ritonavir (20 mg pomotrelvir + 100 mg ritonavir, single dose; 50 mg pomotrelvir + 100 mg ritonavir, once daily for 10 days). Treatment difference was expressed using geometric mean ratios (GMRs) and their 90% confidence intervals (CIs).

Safety and tolerability assessment

Safety and tolerability were assessed throughout the study period by monitoring and recording adverse events, physical examination findings, clinical laboratory tests, vital signs, urine drug and alcohol assessments, calculated

creatinine clearance, serum/urine pregnancy tests (females of childbearing potential only), and 12-lead electrocardiogram results. SARS-CoV-2, hepatitis B virus, hepatitis C virus, and HIV-1 testing were performed during screening.

PBPK

A PBPK model for pomotrelvir based on in vitro and in vivo information on the metabolism and PK of pomotrelvir was constructed in the Simcyp Simulator (V21 Release 1) following the workflow shown in [Figure S1](#). The model was developed to simulate plasma concentration–time profiles of pomotrelvir following a single dose and repeat dosing in healthy subjects and then applied to evaluate the likely impact of administration of strong (itraconazole), moderate (fluconazole and erythromycin), and weak (cimetidine) CYP3A4 inhibitors and strong (rifampicin) and moderate (efavirenz) CYP3A4 inducers on the PK of pomotrelvir and the potential for CYP1A2-, CYP2B6-, CYP2C8-, CYP2C9-, CYP2C19-, and CYP3A4-mediated DDIs with pomotrelvir as a perpetrator (inhibitor or inducer for the CYP enzyme activity).

Distribution

The PBPK model for pomotrelvir was developed using a full-body PBPK model. Tissue-to-plasma partition coefficient values were predicted using the methodology described by Poulin and Theil¹² and updated by Berezhkovskiy¹³ using LogP or LogD (lipid/water partitioning coefficient) and protein binding as input.

Absorption

Absorption was described by a mechanistic absorption model (Simcyp Advanced Dissolution, Absorption and Metabolism [ADAM] model). In human colon adenocarcinoma clone 2 (Caco-2) and Madin Darby canine kidney–breast cancer resistance protein (BCRP) cell lines, pomotrelvir exhibits poor apparent permeability with measurements of 0.36×10^{-6} cm/s and 1.01×10^{-6} cm/s, respectively, and a large efflux ratio. These in vitro measurements did not adequately predict absorption. Pomotrelvir clinical PK appeared dose proportional over the doses studied when administered with food. In vivo, ritonavir (a potent P-glycoprotein and BCRP efflux transporter inhibitor), when coadministered at 100 mg once a day with pomotrelvir, did not

impact the absorption of pomotrelvir. Thus, the mechanistic effective permeability model was used to predict regional permeability from LogP and molecular weight without considering efflux transporters.

Metabolism

In vivo, pomotrelvir is subject to nonhepatic and likely presystemic hydrolysis, which was thought to contribute ~50% of the apparent clearance of pomotrelvir following oral dosing. As no in vitro data were available to describe this elimination process, presystemic hydrolysis was taken into account by assuming incomplete absorption as was predicted using the ADAM model (predicted absorption fraction at 700 mg is 0.65).

In vitro, pomotrelvir was mainly metabolized by CYP3A4 with CYP2C8, contributing to a minor extent ($fm_{CYP3A4}=88\%$, $fm_{CYP2C8}=11\%$ [fm , fraction metabolism]) (Appendix S1). A clinical study was performed in combination with ritonavir. The dose-normalized effect of ritonavir on the systemic exposure (AUC) of pomotrelvir was minimal, indicating the contribution of CYP3A4 to the metabolism of pomotrelvir was less than 88%. Using a mean apparent oral clearance value of 33.19 L/h derived from clinical studies where pomotrelvir was investigated after an oral dose of 300 mg administered with food (FIH study) and a fm_{CYP3A4} value of 25% to match the ritonavir DDI study, the retrograde model (extrapolation from in vivo data) was used to estimate an unbound intrinsic clearance ($Cl_{int,u}$) to match the observed data. The $Cl_{int,u}$ value was apportioned to CYP3A4 and non-CYP3A4 to obtain estimates of 0.376 μ L/min/pmol CYP3A4 and 137.91 μ L/min/mg protein (additional undefined $Cl_{int,u}$). The additional undefined value represents the hydrolysis and any CYP2C8 metabolism. Renal clearance (CL_r) was negligible in preclinical species so was assumed negligible ($Cl_r=0$) in the model.

Changes in enzyme kinetics attributed to enzyme inhibition and induction

Following incubation with human liver microsome (HLM), pomotrelvir exhibited weak to moderate inhibition of CYP1A2, CYP2C8, CYP2C9, CYP2C19, CYP2D6, and CYP3A4 (Appendix S1). The concentration to reduce enzyme activity to 50% of the uninhibited values were adjusted to an inhibition constant (K_i ; concentration required to produce half maximum inhibition) value using the Cheng-Prusoff equation and incorporated into the model. Pomotrelvir is a mechanism-based inhibitor and inducer of CYP3A4, therefore autoinhibition and

autoinduction were integrated in the PBPK model. It should be noted that mechanism-based inhibition (MBI) is typically overpredicted and that in vitro appearance K_i (μM) values often have to be optimized to recover observed DDIs. The f_u (fraction unbound in HLM) value for CYP3A4 MBI parameters was optimized to correctly predict the observed PK after multiple doses of pomotrelvir and to account for the observed impact of the coadministration of pomotrelvir on the exposure of midazolam.

In in vitro induction experiments in human hepatocytes at concentrations from 0.3 to 30 μM , pomotrelvir increased CYP1A2, CYP2B6, CYP2C8, CYP2C9, CYP2C19, and CYP3A4 mRNA by at least twofold (Appendix S1). Given that no clear dose response was observed in the

CYP1A2, CYP2C8, CYP2C9, and CYP2C19 in vitro induction studies, it was not possible to calculate a concentration with the maximum induction effect and a concentration with 50% of the maximum induction effect for these CYPs with a high level of confidence. Thus, only induction parameters for CYP2B6 and CYP3A4 were included in the model.

All final parameters used for the simulation of pomotrelvir kinetics are listed in Table 1.

Population characteristics

The healthy volunteer (HV) population available within the Simcyp Simulator (V21 Release 1) was used in this

TABLE 1 Final input parameters for pomotrelvir in physiologically-based pharmacokinetic modeling.

Parameter	Value	Parameter	Value
Molecular weight (g/mol)	455.94	CYP1A2 K_i (μM)	9.045
LogP	3	CYP2C8 K_i (μM)	1.93
Compound type	Neutral	CYP2C9 K_i (μM)	12.28
B:P	0.93	CYP2C19 K_i (μM)	27.325
f_u	0.044	CYP2D6 K_i (μM)	25.37
Main binding protein	HSA	CYP3A4 K_i (μM)	34.71
$f_{u_{\text{gut}}}$	0.044	$f_{u_{\text{mic}}}$	0.85
$P_{\text{trans},0}$ (pred) ($\times 10^{-6}$ cm/s)	4708.8	CYP3A4 K_{app} (μM)	14.75
$P_{\text{eff},\text{man}}$ (pred) ($\times 10^{-4}$ cm/s)	16.871	CYP3A4 K_{inact} (1/h)	3.72
Q_{gut} (L/h)	8.5293	$f_{u_{\text{mic}}}$	0.85
Formulation type	Solution with precipitation	CYP2B6 Ind_{max} (μM)	6.67
Aqueous phase solubility	Solubility at pH	CYP2B6 IndC_{50} (μM)	4.836
Solubility pH	6.71	CYP3A4 Ind_{max}	16
Solubility (mg/mL)	0.01	CYP3A4 IndC_{50} (μM)	2.096
V_{ss} (L/kg)	1.81		
K_p scalar	1		
CL/F (L/h)	33.19		
$f_{\text{m}_{\text{CYP3A4}}}$	0.25		
CYP3A4 CL_{int} ($\mu\text{L}/\text{min}/\text{pmol}$)	0.376		
Additional HLM CL_{int} ($\mu\text{L}/\text{min}/\text{mg}$)	137.91		
CL_R (L/h)	0		

Abbreviations: B:P, blood-to-plasma ratio; CL/F, apparent oral clearance; CL_{int} , intrinsic metabolic clearance; CL_R , renal clearance; CYP, cytochrome P450; f_{m} , fraction of drug metabolized; f_u , fraction unbound in plasma; $f_{u_{\text{mic}}}$, free fraction of drug in an in vitro microsomal preparation; HLM, human liver microsome; HSA, human serum albumin; IndC_{50} , inducer concentration that supports half maximal induction; Ind_{max} , maximal fold induction over vehicle; K_{app} , apparent enzyme inhibition constant; K_i , enzyme competitive inhibition constant; K_{inact} , inactivation rate of enzyme; K_p scalar, tissue-plasma partition coefficient scalar; LogP, log of the octanol–water partition coefficient for the neutral compound; $P_{\text{eff},\text{man}}$ (pred), predicted effective human jejunum permeability; $P_{\text{trans},0}$ (pred), predicted permeability; Q_{gut} , flow rate for overall delivery of drug to the gut (drug dependent); V_{ss} , volume of distribution at steady state.

analysis. Except for demographic data collected in the clinic (FIH study), all other parameter values for the HV population are the same as those used for the Caucasian population. Default Simcyp parameter values for creating a virtual North European Caucasian population (physiological parameters including liver volume, blood flows, and enzyme abundances) have been described previously.¹⁴

Simulations

For the model development and verification, 10 simulated trials of virtual subjects with characteristics that matched (according to the number, age range, and proportion males and females) with those of the subjects used in each clinical study were generated.

To evaluate the likely impact of administration of CYP3A4 inhibitors and inducers, 10 virtual trials of 10 healthy subjects (50% female) aged 20–50 years receiving a single oral dose of 700 mg pomotrelvir in the absence of perpetrator and on the seventh day of 16 days of oral dosing of perpetrator were generated.

To assess the CYP1A2-, CYP2B6-, CYP2C8-, CYP2C9-, CYP2C19-, and CYP3A4-mediated DDIs, victim (impacted by inhibitors or inducers for the CYP enzymes) drugs were administered as a single dose with and without coadministration of pomotrelvir. All simulations were performed under steady-state conditions for pomotrelvir. A total of 10 virtual trials of 10 healthy subjects (50% female) aged 20–50 years receiving a single oral dose of 150 mg substrate in the absence of pomotrelvir and on the seventh day of 11 days of dosing of pomotrelvir (700 mg b.i.d.) were generated.

In a recent publication, Kilford et al.¹⁵ recommended a sensitivity analysis using an appropriate range of K_i values when no significant DDIs are predicted to assess the worst-case scenario for DDI risk.

Additional DDI simulations were therefore performed after reducing the unbound K_i values by 10-fold. The objective of this sensitivity analysis was to account for the worst-case scenario of potentially inaccurate enzyme K_i estimates from in vitro experiments and other uncertainties.

The impact of pomotrelvir on the exposure of the representative oral hormonal contraceptive drugs ethinyl estradiol and levonorgestrel was evaluated in two separate simulations. In each of the two simulations, 10 virtual trials of 10 healthy subjects (100% female) aged 18 to 45 years receiving a single oral dose of 0.035 mg ethinyl estradiol, or 0.27 mg levonorgestrel, in the absence of pomotrelvir and on the seventh day of 11 days of dosing of pomotrelvir (700 mg b.i.d.) were generated.

RESULTS

In vitro assays

In vitro data indicate that pomotrelvir is a substrate for human CYP3A4 and CYP2C8, which are responsible for 88% and 11% of the hepatic metabolism of pomotrelvir, respectively. No inhibitory effect on CYP2B6, CYP2C19, or CYP2D6 was observed for pomotrelvir in vitro, whereas a weak to moderate inhibition for CYP1A2, CYP2C9, and CYP2C8 and time-dependent inhibition (TDI) for CYP3A4 was shown. In addition, pomotrelvir has shown an induction effect for CYP2B6 and CYP3A4, but has no clear concentration-dependent induction effect on CYP1A2, CYP2C8, CYP2C9, or CYP2C19 in vitro (detailed results are in Appendix S1).

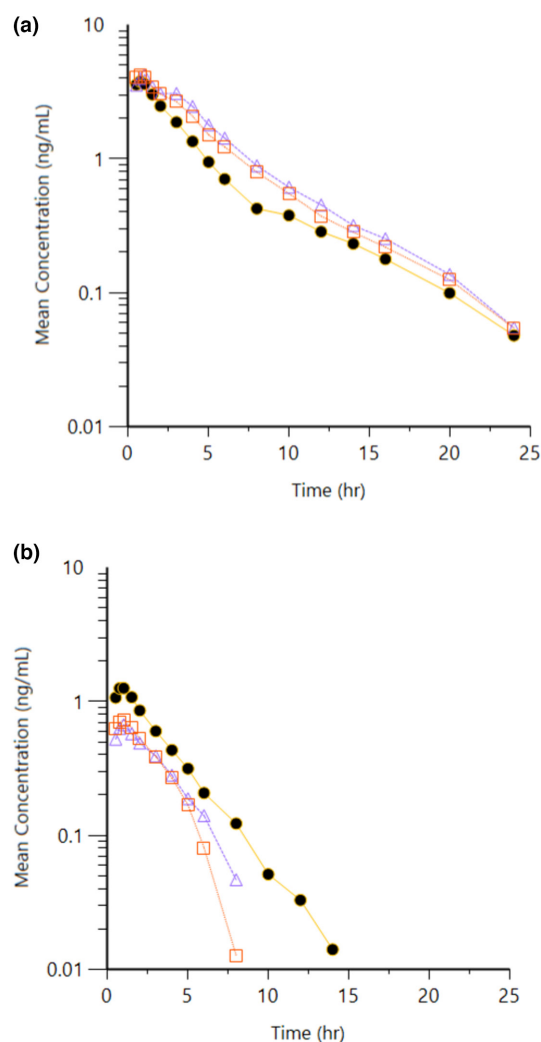


FIGURE 1 Mean (standard deviation) plasma concentrations of (a) midazolam and (b) 1-hydroxy-midazolam versus time when administered alone (solid circle) or coadministered with pomotrelvir (Day 6 with open triangle, Day 11 with open square).

With the weak to moderate potential inhibition or induction effect observed for pomotrelvir in vitro and the results from the basic static model analysis, the DDI potential mediated by CYP1A2, CYP2B6, CYP2C8, CYP2C9, CYP2C19, and CYP3A4 enzymes were further evaluated in PBPK modeling and simulation and in clinic for CYP3A4 because of the potential complex DDI effect that could involve TDI and induction for pomotrelvir as a perpetrator as well as a victim.

Clinical midazolam study

The mean plasma concentration–time profile of midazolam and its metabolite 1-OH-midazolam are plotted in Figure 1. All predose concentrations of midazolam were below the lower limit of quantitation on all occasions, demonstrating that the wash-out period was adequate. After a single dose of midazolam, mean plasma concentrations of midazolam were slightly higher, and the concentration of 1-OH-midazolam was lower, following coadministration of pomotrelvir on Days 6 and 10 than administered alone on Day 1. The plasma exposures of midazolam and 1-OH-midazolam were compared between

that after coadministration with a supratherapeutic dose at 1050 mg b.i.d. pomotrelvir versus administration alone. The GMR with 90% CI for AUC_{last} , AUC_{inf} , and C_{max} (Table 2) showed that the systematic exposure of midazolam increased, and 1-OH-midazolam decreased, by <50% after coadministration with pomotrelvir compared with midazolam alone.

Clinical ritonavir study

The pomotrelvir FIH study included two DDI cohorts to evaluate the potential impact of ritonavir, an inhibitor of CYP3A4, on pomotrelvir PK. In one of the cohorts, pomotrelvir 20 mg was coadministered with 100 mg ritonavir as a single dose, whereas in the other cohort, pomotrelvir 50 mg was coadministered with ritonavir 100 mg once daily for 10 days. A comparison of pomotrelvir plasma exposure following coadministration of 100 mg ritonavir with that after pomotrelvir administered alone at a 100 mg single dose (the evaluated pomotrelvir dose level that was the closest to that tested in the DDI cohorts in the FIH study) was performed, and the GMR with 90% CI for $AUC_{last}/dose$, $AUC_{inf}/dose$, and $C_{max}/dose$ of pomotrelvir

TABLE 2 Statistical comparisons of midazolam plasma exposure following midazolam coadministration with pomotrelvir (1050 mg twice daily) versus midazolam alone.

PK parameter	Geometric mean		Geometric mean ratio (MDZ + POMO)/(MDZ)	90% CI
	MDZ (N = 8)	MDZ + POMO (N = 8)		
Midazolam				
	Day 1	Day 6		
C _{max} (ng/mL)	4.06	4.44	1.09	0.91, 1.32
AUC _{last} (h*ng/mL)	15.1	22.7	1.51	1.18, 1.92
AUC _{inf} (h*ng/mL)	16.2	24.0	1.48	1.16, 1.80
	Day 1	Day 11		
C _{max} (ng/mL)	4.06	4.44	1.09	0.87, 1.37
AUC _{last} (h*ng/mL)	15.1	20.7	1.36	1.05, 1.78
AUC _{inf} (h*ng/mL)	16.2	21.8	1.33	1.02, 1.74
1-OH-midazolam				
	Day 1	Day 6		
C _{max} (ng/mL)	1.36	0.73	0.53	0.41, 0.7
AUC _{last} (h*ng/mL)	4.72	2.87	0.62	0.49, 0.78
AUC _{inf} (h*ng/mL)	4.76	3.09	0.65	0.49, 0.85
	Day 1	Day 11		
C _{max} (ng/mL)	1.36	0.8	0.58	0.45, 0.76
AUC _{last} (h*ng/mL)	4.72	2.64	0.56	0.44, 0.72
AUC _{inf} (h*ng/mL)	4.76	2.66	0.56	0.43, 0.72

Abbreviations: 1-OH-midazolam, 1-hydroxy-midazolam; AUC_{inf} , area under the curve from time 0 to infinity; AUC_{last} , area under the curve from time 0 to the last quantifiable concentration; CI, confidence interval; C_{max} , maximum observed concentration; MDZ, midazolam; PK, pharmacokinetics; POMO, pomotrelvir.

TABLE 3 Comparisons of POMO dose-normalized plasma exposure following coadministration with 100 mg RTV versus POMO alone.

PK parameters	GMR (90% CI) (20 mg PBI + 100 mg RTV, SD) / (100 mg POMO, SD)	GMR (90% CI) (50 mg PBI + 100 mg RTV, Day1)/(100 mg POMO, SD)	GMR (90% CI) (50 mg PBI + 100 mg RTV, Day5)/(100 mg POMO, SD)	GMR (90% CI) (50 mg PBI + 100 mg RTV, Day10)/(100 mg POMO, SD)
AUC _{inf} /dose, (ng*h/mL)/mg	0.92 (0.67, 1.26)	1.54 (1.13, 2.1)	1.34 (0.96, 1.87) ^a	1.37 (1.05, 1.79) ^b
AUC _{last} /dose, (ng*h/mL)/mg	1.06 (0.68, 1.65)	1.38 (1.08, 1.76)		
C _{max} /dose, (ng/mL)/mg	0.97 (0.76, 1.22)	1.46 (1.16, 1.84)	1.3 (0.9, 1.89)	1.41 (1.05, 1.91)

Abbreviations: AUC_{inf}, area under the curve from time 0 to infinity; AUC_{last}, area under the curve from time 0 to the last quantifiable concentration; CI, confidence interval; C_{max}, maximum observed concentration; GMR, geometric mean ratio; PK, pharmacokinetics; POMO, pomotrelvir; RTV, ritonavir; SD, single dose.

^aGMR was for [AUC_{last}/Dose of (50 mg PBI + 100 mg RTV, Day5)]/[AUC_{inf}/Dose (100 mg POMO, SD)].

^bGMR was for [AUC_{last}/Dose of (50 mg PBI + 100 mg RTV, Day10)]/[AUC_{inf}/Dose (100 mg POMO, SD)].

coadministered with ritonavir versus pomotrelvir alone was estimated (Table 3). The data demonstrated that the dose-normalized systemic exposure of pomotrelvir increased modestly (0.92–1.54-fold) in the presence of ritonavir.

PBPK

Model development and verification

Simulated PK profiles, AUC_{inf}, AUC over the dosing interval, and C_{max} of pomotrelvir following single and repeat oral doses of pomotrelvir (100 mg to 2100 mg) to healthy subjects were in reasonable agreement with the observed data (all within twofold, the majority within 1.5-fold) from the FIH clinical study (Table S3, Figure 2).

The simulated AUC_{inf} and C_{max} following the coadministration of a single dose of 100 mg ritonavir with 20 mg pomotrelvir, or following repeated daily coadministration of 100 mg ritonavir with 50 mg pomotrelvir, were in reasonable agreement with the observed data (all within twofold difference) given the observed clinical data variability (Table S4). The model was also able to accurately predict the effect of pomotrelvir (1050 mg b.i.d.) on the exposure of midazolam (Day 6 and Day 11) to be within 1.3-fold of the observed data (data not shown).

Pomotrelvir as perpetrator

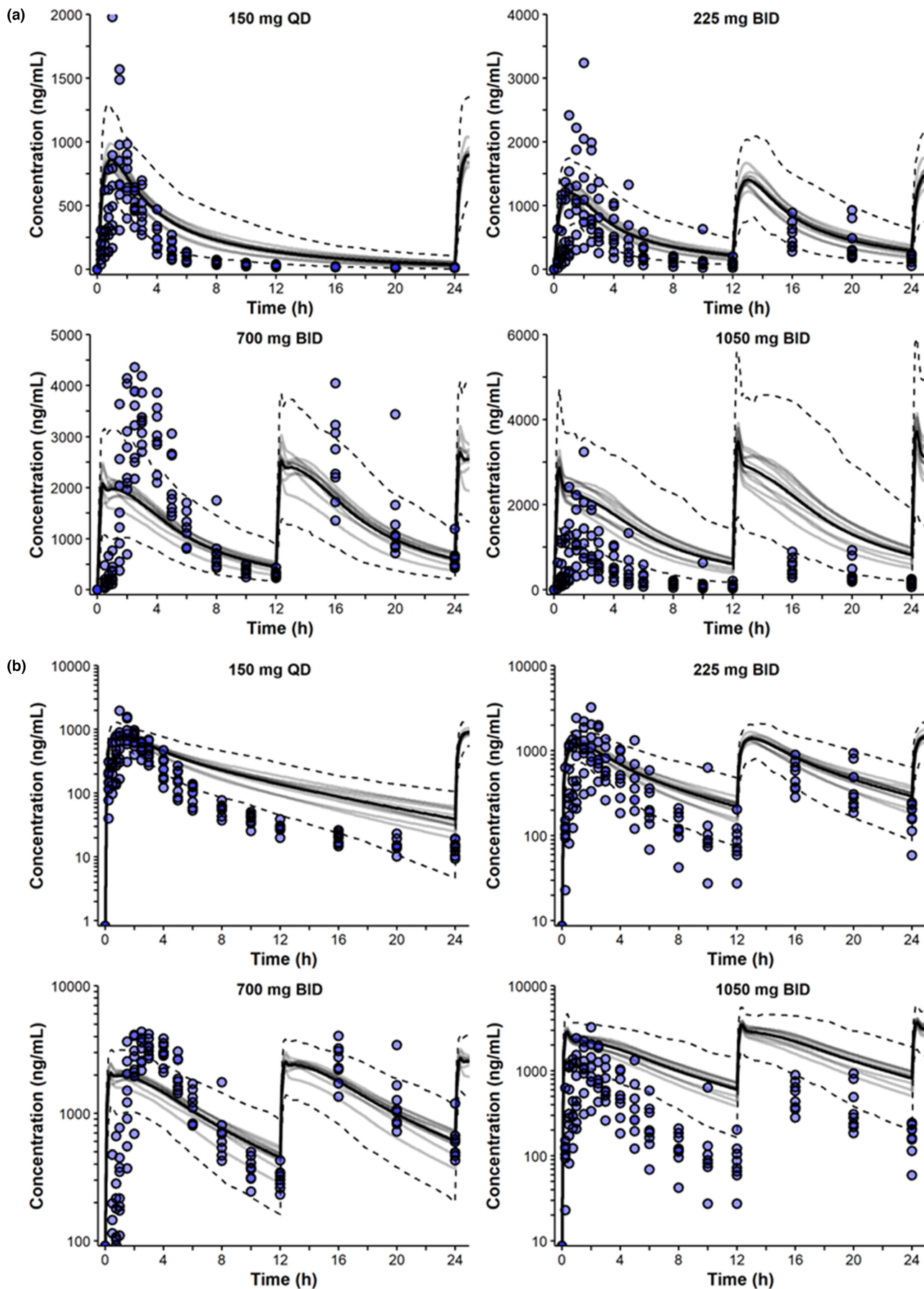
In this PBPK analysis, no clinically significant DDIs were predicted following the administration of multiple doses of the proposed pomotrelvir daily dose of 700 mg b.i.d. with the sensitive probe substrates for CYP1A2, CYP2B6, CYP2C8, CYP2C9, and CYP2C19. The sensitivity analysis with 10-fold reduction of K_i for these CYP enzymes predicted a weak inhibition effect on CYP2C8 only with the simulated geometric mean AUC_{inf} and C_{max} ratio (with vs without pomotrelvir) at 1.55 and 1.36, respectively. Moreover, consistent with the clinical DDI data, a weak inhibitory effect was predicted in silico with the sensitive CYP3A4 substrate midazolam (Table 4).

No clinically significant DDIs were predicted following administration of multiple doses of 700 mg b.i.d. PBI-0451 with ethinyl estradiol and levonorgestrel. Specifically, the simulated AUC_{inf} and C_{max} values, with and without pomotrelvir, were <1.20-fold under simulated steady-state conditions for these oral contraceptives (Table 4).

Pomotrelvir as victim

This analysis indicated that the simulated changes in plasma exposure of pomotrelvir during administration with strong inhibitors of CYP3A4 (itraconazole) to healthy subjects are weak. No clinically significant DDIs were predicted with moderate and weak CYP3A4 inhibitors.

FIGURE 2 Linear (a) and log-linear (b) simulated and observed plasma concentration–time profiles of the first oral dose (Day 1) of 150 mg pomotrelvir every day (QD) and 225, 700, and 1050 mg pomotrelvir twice daily (BID) for 10 days in healthy subjects. Depicted are simulated (lines) and observed data (circles, $n = 8$; first-in-human study). The gray lines represent the mean values of simulated individual trials, the dashed lines represent the 5th and 95th percentiles, and the solid black line represents the mean data for the simulated population ($n = 80$).



A weak impact on the exposure of pomotrelvir was predicted in the presence of strong or moderate CYP3A4 inducers (Table 5).

DISCUSSION

The CYP enzyme-mediated DDI potential for pomotrelvir was evaluated in in vitro studies, where the CYP isoforms that are responsible for hepatic metabolism of pomotrelvir were identified. In addition, the inhibitory and inducing effects of pomotrelvir on major CYP enzymes were evaluated. The inhibitory effect observed in vitro was interpreted using a basic model, which was

TABLE 4 Summary of simulated geometric mean AUC_{inf} and C_{max} ratios for sensitive CYP probe substrates and representative oral contraceptive drugs in the absence and presence of repeat oral dosing of 700 mg pomotrelvir twice daily in healthy subjects (physiologically-based pharmacokinetic evaluation).

Substrate	GMR	
	AUC_{inf}/AUC_t	C_{max}
CYP1A2 Caffeine	1.01	1.00
CYP2B6 Bupropion	0.97	0.98
CYP2C8 Repaglinide	1.16 ^a	1.11
CYP2C9 Tolbutamide	1.01	1.00
CYP2C19 Omeprazole	1.08 ^a	1.03
CYP3A4 Midazolam	1.54	1.23
Oral contraceptive drugs		
Ethinyl estradiol	1.09	1.03
Levonorgestrel	1.16	1.02
Sensitivity analysis–10-fold lower $K_{i,u}$		
CYP1A2 Caffeine	1.13	1.04
CYP2C8 Repaglinide	1.55	1.36
CYP2C9 Tolbutamide	1.08	1.03
CYP2C19 Omeprazole	1.14 ^a	1.06

Abbreviations: AUC_{inf} , area under the curve from time 0 to infinity; AUC_t , area under the curve over the dosing interval (time = 24 h); C_{max} , maximum observed concentration; CYP, cytochrome P450; GMR, geometric mean ratio; $K_{i,u}$, unbound enzyme competitive inhibition constant.

^aRatio was calculated using AUC_t (AUC_t , area under the curve over the dosing interval [time = 24 h]).

anticipated to overestimate the effect because the model was based on the maximum clinical pomotrelvir exposure (C_{max}). Furthermore, a dynamic mechanism-based PBPK model was successfully developed with a validation showing similar PK results between the simulated data and that observed in clinic and applied to predict the clinical DDI potential that could be caused by pomotrelvir being a perpetrator or a victim. In addition, the potential DDI of pomotrelvir through the CYP3A4 pathway was evaluated in the clinic by coadministration with midazolam and ritonavir.

Pomotrelvir DDI potential as a victim

In vitro data indicated that pomotrelvir was a substrate for human CYP3A4 (major, fm 88%) and 2C8 (minor, fm 11%), whereas the contribution of the CYP isoforms 1A2, 2A6, 2B6, 2C9, 2C19, 2D6, 2E1, and 3A5 to pomotrelvir metabolism was negligible. Despite pomotrelvir being turned over in vitro by CYP3A4, clinically upon single or multiple doses of coadministration with ritonavir, pomotrelvir had a minimal increase (<50%) in exposure, suggesting that pomotrelvir is not a sensitive substrate for CYP3A4 in humans that would be associated with a clinically significant DDI with inhibitors or inducers of this pathway. Based on the available knowledge on the clearance mechanism and the role of CYP3A4 and CYP2C8, the clinical DDI liability attributed to CYP2C8 is not expected to be significant. Overall, the results suggest that pomotrelvir is not a sensitive substrate of CYP3A4 or CYP2C8 in humans and is not expected to have substantial changes in exposure when

TABLE 5 Summary of simulated geometric mean AUC_{inf} and C_{max} ratios for pomotrelvir in the absence and presence of CYP3A4 inhibitors and inducers in healthy subjects following single oral dosing of 700 mg pomotrelvir (physiologically-based pharmacokinetic evaluation).

Perpetrator	Single dose (700 mg pomotrelvir)	
	AUC_{inf} GMR	C_{max} GMR
CYP3A4 inhibitors (strength of inhibitor)		
Itraconazole (strong)	1.32	1.10
Fluconazole (moderate)	1.20	1.07
Erythromycin (moderate)	1.19	1.07
Cimetidine (weak)	1.05	1.02
CYP3A4 inducers (strength of inducer)		
Rifampicin (strong)	0.52	0.76
Efavirenz (moderate)	0.67	0.84

coadministered with DDI perpetrators of these enzymatic pathways.

Pomotrelvir DDI potential as a perpetrator

Pomotrelvir showed the potential to reversibly and time-dependently inhibit as well as induce CYP3A4 in vitro, whereas midazolam had a minimal (<50%) increase in exposure in humans when codosed with pomotrelvir at multiday doses of 1050 mg b.i.d., thus suggesting a potential weak inhibitory net effect of pomotrelvir for CYP3A4. Based on in vitro and PBPK modeling and simulation assessment, no clinically significant DDIs were predicted following the administration of multiple doses of the proposed daily pomotrelvir dose of 700 mg b.i.d. with sensitive probe substrates for CYP1A2, CYP2B6, CYP2C8, CYP2C9, or CYP2C19. In addition, no clinically significant DDIs were predicted with the oral hormonal contraceptive drugs ethinyl estradiol and levonorgestrel. The evaluation of the two main metabolites, PBI-0451A and S4-Q1, did not result in reversible inhibition for the activity of the tested CYP enzymes in vitro at clinically relevant concentrations (Appendix S1). Overall, these results suggest that pomotrelvir at the proposed clinical dose of 700 mg b.i.d. is not anticipated to have clinically meaningful DDI potential with the substrates of major CYP enzymes.

Study limitation

The PBPK model was developed at the early phase of drug development, when the absorption, distribution, metabolism, and excretion of the compound in human was not yet fully understood, therefore there were a number of uncertainties with the current model. The mechanisms underlying the elimination of pomotrelvir still need to be clarified. It was believed that presystemic hydrolysis played a significant role in the clearance of pomotrelvir, but the relative contribution of this pathway was unclear. The calculation of CYP3A4 fm was influenced by the weak DDI observed with ritonavir, but hampered by the variability in the clinical data and the noncrossover study design. In addition, there was some indication of induction in human hepatocytes with CYP1A2 and the CYP2C enzymes, which could counteract any inhibition observed with these enzymes; however, quantifiable data were not available to add these mechanisms into the model. Despite the limitations during the modeling, the recent human mass balance study using radiolabeled pomotrelvir¹⁶ suggested that nonhepatic hydrolysis of pomotrelvir is the major route of metabolism and clearance for pomotrelvir. Minimal urinary excretion of intact pomotrelvir and a low

percentage of phase I oxidative metabolites observed in excreta support the settings of negligible urinary excretion and low CYP3A4 fm in the PBPK model.

Based on the comprehensive in vitro, in vivo (in clinic), and in silico (PBPK) evaluations, pomotrelvir is anticipated to have no clinically meaningful CYP enzyme-mediated DDI potential at a clinical dose of 700 mg b.i.d. This favorable DDI profile supported the recommendation to not exclude any patients as a result of CYP-mediated DDI concerns in pomotrelvir phase II clinical trials. Given the role of non-CYP-mediated mechanisms in the clearance of pomotrelvir, additional clinical DDI studies may not be necessary. The DDI assessment approach of including small DDI cohorts in the FIH study coupled with PBPK modeling and simulation provides an early read on DDI potential in early drug development. This approach supported removing restrictions for use of concomitant medications in clinical trials and also reduced the need for additional DDI clinical studies, thereby reducing unnecessary exposure to DDI study drugs in HIVs.

AUTHOR CONTRIBUTIONS

Z.Y., L.V., N.R., H.M.J., D.W., and B.P.K. wrote the manuscript. B.P.K., Z.Y., A.P., N.R., L.V., and H.M.J. designed the research. Z.Y., D.C., A.P., N.R., L.V., and H.M.J. performed the research. Z.Y., L.V., N.R., H.M.J., and D.W. analyzed the data.

ACKNOWLEDGMENTS

The authors thank the participants in this study; the personnel at Novotech, Pharmaron, QPS, LLC and WuXi AppTec who were involved in the conduct of this study; and Pardes colleagues for editorial support.

FUNDING INFORMATION

No funding was received for this work.

CONFLICT OF INTEREST STATEMENT

Z.Y., D.C., A.P., D.W., and B.P.K. were employees of Pardes Biosciences, Inc. and may hold stock or stock options in the company. N.R., L.V., and H.M.J. are employees of Certara Inc. and may hold stock in the company.

ORCID

David Wilfret  <https://orcid.org/0009-0003-9068-8231>

REFERENCES

1. Barouch DH. COVID-19 vaccines—immunity, variants, boosters. *N Engl J Med*. 2022;387:1011-1020.
2. Niknam Z, Jafari A, Golchin A, et al. Potential therapeutic options for COVID-19: an update on current evidence. *Eur J Med Res*. 2022;27(1):6.

3. Callender LA, Curran M, Bates SM, Mairesse M, Weigandt J, Betts CJ. The impact of pre-existing comorbidities and therapeutic interventions on COVID-19. *Front Immunol*. 2020;11:1991.
4. Pfizer Inc. *PAXLOVID (nirmatrelvir tablets; ritonavir tablets) [emergency use authorization]*. Pfizer Inc; 2023. Accessed March 21, 2023. Available from: <https://www.fda.gov/media/155050/download>
5. Gold JAW, Kelleher J, Magid J, et al. Dispensing of oral antiviral drugs for treatment of COVID-19 by zip code-level social vulnerability—United States, December 23, 2021–May 21, 2022. *MMWR Morb Mortal Wkly Rep*. 2022;71:825-829.
6. Kwong A, Tong X, Borroto-Esoda K, et al. Discovery and development of PBI-0451: a novel oral protease inhibitor for the potential treatment of SARS-CoV-2. Poster presented at: *The World Antiviral Congress* 2022. November 28–December 1, 2022; San Diego, CA.
7. Kearney BP, Plummer A, Wolfgang G, et al. PBI-0451: an orally administered 3CL protease inhibitor of SARS-CoV-2 for COVID-19. Poster presented at: *The 29th CROI Annual Conference*. February 12–16, 2022. Virtual meeting.
8. Jean D, Naik K, Milligan L, et al. Development of best practices in physiologically based pharmacokinetic modeling to support clinical pharmacology regulatory decision-making—a workshop summary. *CPT Pharmacometrics Syst Pharmacol*. 2021;10(11):1271-1275.
9. Food and Drug Administration. In vitro drug interaction studies – cytochrome P450 enzyme- and transporter-mediated drug interactions guidance for industry. 2020 Available from: <https://www.fda.gov/regulatory-information/search-fda-guidance-documents/in-vitro-drug-interaction-studies-cytochrome-p450-enzyme-and-transporter-mediated-drug-interactions>
10. Denisov IG, Grinkova YV, Camp T, McLean MA, Sligar SG. Midazolam as a probe for drug-drug interactions mediated by CYP3A4: homotropic allosteric mechanism of site-specific hydroxylation. *Biochemistry*. 2021;60:1670-1681.
11. Loos NHC, Beijnen JH, Schinkel AH. The mechanism-based inactivation of CYP3A4 by ritonavir: what mechanism? *Int J Mol Sci*. 2022;23:9866.
12. Poulin P, Theil FP. Prediction of pharmacokinetics prior to in vivo studies. 1. Mechanism-based prediction of volume of distribution. *J Pharm Sci*. 2002;91:129-156.
13. Berezhkovskiy LM. Volume of distribution at steady state for a linear pharmacokinetic system with peripheral elimination. *J Pharm Sci*. 2004;93:1628-1640.
14. Howgate EM, Rowland Yeo K, Proctor NJ, Tucker GT, Rostami-Hodjegan A. Prediction of in vivo drug clearance from in vitro data. I: impact of inter-individual variability. *Xenobiotica*. 2006;36:473-497.
15. Kilford PJ, Chen KF, Crewe K, et al. Prediction of CYP-mediated DDIs involving inhibition: approaches to address the requirements for system qualification of the Simcyp simulator. *CPT Pharmacometrics Syst Pharmacol*. 2022;11:822-832.
16. Yang Z, Wong SL, Cha D, et al. Characterization of pharmacokinetics, biotransformation and elimination of pomotrelvir orally administered in healthy male subjects using two [¹⁴C]-labeled microtracers with separate labeling positions. Submitted.

SUPPORTING INFORMATION

Additional supporting information can be found online in the Supporting Information section at the end of this article.

How to cite this article: Yang Z, Rioux N, Vincent L, et al. A comprehensive evaluation in clinic and physiologically-based pharmacokinetic modeling and simulation to confirm lack of cytochrome P450-mediated drug–drug interaction potential for pomotrelvir. *CPT Pharmacometrics Syst Pharmacol*. 2023;12:1553-1564. doi:[10.1002/psp4.13034](https://doi.org/10.1002/psp4.13034)